

Integrated taxonomy unveils new species of Trigonalyidae (Insecta, Hymenoptera) from Yunnan, China

Bing-Lan Zhang¹, Cheng-Jin Yan^{2,3}, Cornelis van Achterberg^{4,5},
Yan-Qiong Peng⁶, Hua-Yan Chen⁷

1 School of Life Sciences, Sun Yat-sen University, Guangzhou 510275, China **2** Wenzhou Vocational School of Science and Technology, Wenzhou 325300, China **3** Wencheng Modern Agriculture and Health Industry Research Institute, Wenzhou 325300, China **4** State Key Laboratory of Rice Biology and Ministry of Agriculture, Hangzhou 310058, China **5** Key Lab of Agricultural Entomology, Institute of Insect Sciences, Zhejiang University, Hangzhou 310058, China **6** CAS Key Laboratory of Tropical Forest Ecology, Xishuangbanna Tropical Botanical Garden, Chinese Academy of Sciences, Mengla 666303, China **7** Key Laboratory of Plant Resources Conservation and Sustainable Utilization, South China Botanical Garden, Chinese Academy of Sciences, Guangzhou 510650, China

Corresponding authors: Hua-Yan Chen (huayanc@scbg.ac.cn), Cheng-Jin Yan (ycj0685@163.com)

Academic editor: Miles Zhang | Received 6 January 2022 | Accepted 2 March 2022 | Published 29 April 2022

<http://zoobank.org/13EC4891-F124-4E77-BC22-F6978445DAE7>

Citation: Zhang B-L, Yan C-J, van Achterberg C, Peng Y-Q, Chen H-Y (2022) Integrated taxonomy unveils new species of Trigonalyidae (Insecta, Hymenoptera) from Yunnan, China. *Journal of Hymenoptera Research* 90: 101–128. <https://doi.org/10.3897/jhr.90.80150>

Abstract

Trigonalyidae are rarely collected hyperparasitoids that attack the larvae of Ichneumonidae, and Tachinidae associated with phytophagous sawfly or Lepidopteran larvae, or primary endoparasitoids of Vespidae larvae. Trigonalyidae mainly occur in tropical and subtropical regions, but recent studies indicate that they are found to be fairly common in mountainous regions. In this study, DNA barcoding methods based on sequences of the *COI* gene were used to discriminate Trigonalyidae species from Yunnan Province, which is situated in a mountainous area of southwest China. In total, 25 *COI* sequences belonging to 14 morphospecies of four genera were obtained. The intraspecific pairwise distances ranged from 0 to 3.3% and the interspecific pairwise distances ranged from 5.3% to 17.3%. The delimitations of all studied species are congruent with the morphological identification results in both ABGD and bPTP methods. Based on both morphological and molecular analyses, four species from Yunnan are described as new: *Jezonogonalos eburnalva* Zhang & Chen, **sp. nov.**, *Lycogaster umbonata* Chen & van Achterberg, **sp. nov.**, *Taeniogonalos albidorsalis* Zhang & Chen, **sp. nov.**, and *T. paradoxica* Zhang & Chen, **sp. nov.**

Keywords

DNA barcoding, hyperparasitoid, *Jezonogonalos*, *Lycogaster*, parasitoid, *Taeniogonalos*

Introduction

Trigonalidae (Hymenoptera, Trigonalioidea) are rarely collected parasitoid wasps with more than 120 described species in 16 genera worldwide (Carmean and Kimsey 1998; Smith and Stocks 2005; Santos et al. 2012; Smith and Tripotin 2012; Smith et al. 2012; Chen et al. 2014; Yamane 2014; Smith and Tripotin 2015; Tan et al. 2017; Lelej 2019; Chen et al. 2020a). These wasps are thought to be hyperparasitoids that attack the larvae of Ichneumonoidea (Hymenoptera), and Tachinidae (Diptera) associated with phytophagous primary hosts, mostly sawfly or Lepidopteran larvae. Primary endoparasitism of sawflies may occur, but the parasitoid still acts facultatively as a hyperparasitoid (Clausen 1940; Yamane and Terayama 1983; He and Chen 1986; Weinstein and Austin 1991; Carmean and Kimsey 1998). Secondary endoparasitism of vespid wasp larvae occurs when lepidopteran or symphytan caterpillars, with trigonalid eggs inside, are fed to the larvae and the eggs eventually develop in the wasp larvae (Yamane 2014; Tan et al. 2017; Kim et al. 2020). The peculiar biology of Trigonalidae was reviewed in detail by Clausen (1940), Carmean (1991) and Weinstein and Austin (1991, 1995).

Most species of Trigonalidae occur in tropical and subtropical regions and they are unknown from arctic and alpine habitats (Carmean and Kimsey 1998). However, they were found to be fairly common at 1300–1500 m altitude in the Qinling Mountains of NW China (Tan et al. 2017) and the mountainous regions of Tibet (Chen et al. 2020a). Yunnan Province is situated in a mountainous area, with high elevations in the northwest and low elevations in the southeast. This topography allows snow-capped mountains and true tropical environments to occur in one region, which sustains an extremely high biodiversity and high degree of endemism (Liang 2011). Before this study, 11 species have been recorded from Yunnan. In this study, based on an integrative taxonomic approach that combines molecular and morphological evidence, we add four new species from this region.

Material and methods**Collection and identification**

This work is mainly based on specimens of Trigonalidae collected by sweeping net, yellow pan traps (**YPT**), and mostly Malaise traps (**MT**) set up in China. For the molecular study, specimens of some known species from other provinces are also used. Specimens were identified using the keys of Chen et al. (2014) and Tan et al. (2017).

All the studied specimens are deposited in the Museum of Biology, Sun Yat-sen University, Guangzhou, China (**SYSBM**). Morphological terminology generally follows Chen et al. (2014). Multifocal images of the new species (Figs 2–10) and representatives of the known species (Suppl. material 4: Figs S1–S21) were made using a Nikon SMZ25 microscope with a Nikon DS-Ri 2 digital camera system. Images were then post-processed with Adobe Photoshop CS6.

DNA extraction, amplification, and sequencing

In total, 25 specimens of 14 morphospecies were used for DNA barcoding analysis (see Table 1, detailed collecting data of the sequenced see Suppl. material 1: Table S1). Both female and male specimens were selected for a species when such specimens were available. Genomic DNA was extracted from the right mid leg of each specimen using the DNeasy Blood & Tissue Kit (Qiagen, Hilden, Germany), following the manufacturer's protocols. Following the extraction, the “barcode” region of the mitochondrial cytochrome oxidase subunit 1 (*COI*) was amplified using the LCO1490/HCO2198 primer pair (Folmer et al. 1994). Polymerase chain reactions (PCRs) were performed using Tks Gflex DNA Polymerase (Takara) and conducted in a T100 Thermal Cycler (Bio-Rad). Thermocycling conditions were: an initial denaturing step at 94 °C for 5 min, followed by 35 cycles of 94 °C for 30 s, 50 °C for 30 s, 72 °C for 30 s and an additional extension at 72 °C for 5 min. Amplicons were directly sequenced in both directions with forward and reverse primers on an Applied Biosystems (ABI) 3730XL by Guangzhou Tianyi Huiyuan Gene Technology Co., Ltd. (Guangzhou, China). Chromatograms were assembled with Geneious 11.0.3. All sequences generated from this study are deposited in GenBank (accession numbers see Table 1).

Sequence analysis and molecular species delimitation

All sequences were blasted in the BOLD (Barcode of Life Database, http://www.barcodinglife.org/index.php/IDS_OpenIdEngine) and GenBank. Sequences were aligned using MAFFT v7.470 by the G-INS- I strategy (Kato and Standley 2013). Genetic Kimura-2 parameter (K2P) distances within and between species were calculated in MEGA 7 with pairwise deletion for gaps (Kumar et al. 2016).

Two methods, the Automatic Barcode Gap Discovery (ABGD) and the updated Poisson tree processes model (bPTP), were tested for molecular species delimitation. ABGD is a distance-based method and it sorts the sequences into hypothetical species by partitioning and comparing the difference between sequences to identify a “barcode gap” (Puillandre et al. 2012). The ABGD analysis was performed on the web interface (<http://www.abi.snv.jussieu.fr/public/abgd/>), using the default priors, $P_{min} = 0.001$, $P_{max} = 0.1$, Steps 10, and with barcode relative gap width = 1.00. bPTP is an updated version of the original PTP with Bayesian posterior probability, which tests species boundaries on non-ultrametric phylogenetic trees by detecting significant difference in the number of substitutions between species and within species (Zhang

Table 1. Sequenced taxa and GenBank accession numbers.

Code	Species	Sex	GenBank accession No.
En-419020	<i>Jezonogonalos eburnalva</i> sp. n.	male	OM057963
En-419951	<i>Jezonogonalos jiangliae</i> Chen, van Achterberg, He & Xu	male	OM057964
En-419953	<i>Jezonogonalos jiangliae</i> Chen, van Achterberg, He & Xu	male	OM057965
En-419959	<i>Lycogaster angustula</i> Chen, van Achterberg, He & Xu	male	OM057966
En-419022	<i>Lycogaster umbonata</i> sp. n.	male	OM057967
En-419021	<i>Lycogaster umbonata</i> sp. n.	female	OM057968
En-419955	<i>Orthogonalys elongata</i> Teranishi	female	OM057969
En-419957	<i>Orthogonalys elongata</i> Teranishi	male	OM057970
En-419964	<i>Orthogonalys hirasana</i> Teranishi	female	OM057971
En-419023	<i>Taeniogonalos albidorsalis</i> sp. n.	female	OM057972
En-419958	<i>Taeniogonalos cordata</i> Chen, van Achterberg, He & Xu	female	OM057973
En-419952	<i>Taeniogonalos eurysona</i> Chen & van Achterberg	female	OM057974
En-419960	<i>Taeniogonalos fasciata</i> (Strand)	male	OM057975
En-419967	<i>Taeniogonalos flavoscutellata</i> (Chen)	female	OM057976
En-419961	<i>Taeniogonalos formosana</i> (Bischoff)	female	OM057977
En-419965	<i>Taeniogonalos formosana</i> (Bischoff)	male	OM057978
En-419963	<i>Taeniogonalos formosana</i> (Bischoff)	male	OM057979
En-419025	<i>Taeniogonalos formosana</i> (Bischoff)	male	OM057980
En-419962	<i>Taeniogonalos formosana</i> (Bischoff)	female	OM057981
En-419966	<i>Taeniogonalos formosana</i> (Bischoff)	female	OM057982
En-419950	<i>Taeniogonalos formosana</i> (Bischoff)	female	OM057983
En-419954	<i>Taeniogonalos formosana</i> (Bischoff)	female	OM057984
En-419968	<i>Taeniogonalos formosana</i> (Bischoff)	male	OM057985
En-419956	<i>Taeniogonalos gestroi</i> (Schulz)	male	OM057986
En-419024	<i>Taeniogonalos paradoxica</i> sp. n.	male	OM057987

et al. 2013). For bPTP analysis, a Maximum Likelihood (ML) tree was generated in RAxML v8.2.10 under the GTRGAMMA evolutionary model and performed on the bPTP web server (<https://species.h-its.org/ptp/>), with default parameters. The *COI* sequences of *Schlettererius cinctipes* (Cresson) (Hymenoptera: Stephanidae; GenBank: [GQ502933](#)) were selected as the outgroup because of the close relationship between Scolioidea and Pompiloidea (Peters et al. 2017).

Results

The present study generated 25 *COI* sequences with an average of 670 bp. Voucher specimens of these 25 sequences were subjected to further morphological examination, and 14 species belonging to 4 genera were recognized, including 4 new species described below (Table 1). When blasted in BOLD and GenBank databases, the sequences of *Taeniogonalos formosana* (Bischoff) received close matches with *Taeniogonalos taihorina* (Bischoff) (around 95%). Other species had no close matching sequences in BOLD or NCBI. The K2P distances (Suppl. material 2: Table S2; Suppl. material 3: Table S3) showed a larger intergroup than intragroup distance for the *COI* sequences. The intraspecific pairwise distances ranged from 0 to 3.3%. The interspecific pairwise distances ranged from 5.3% to 17.3%. The delimitations of all studied species are congruent with the morphological identification results in both ABGD and bPTP methods (Fig. 1).

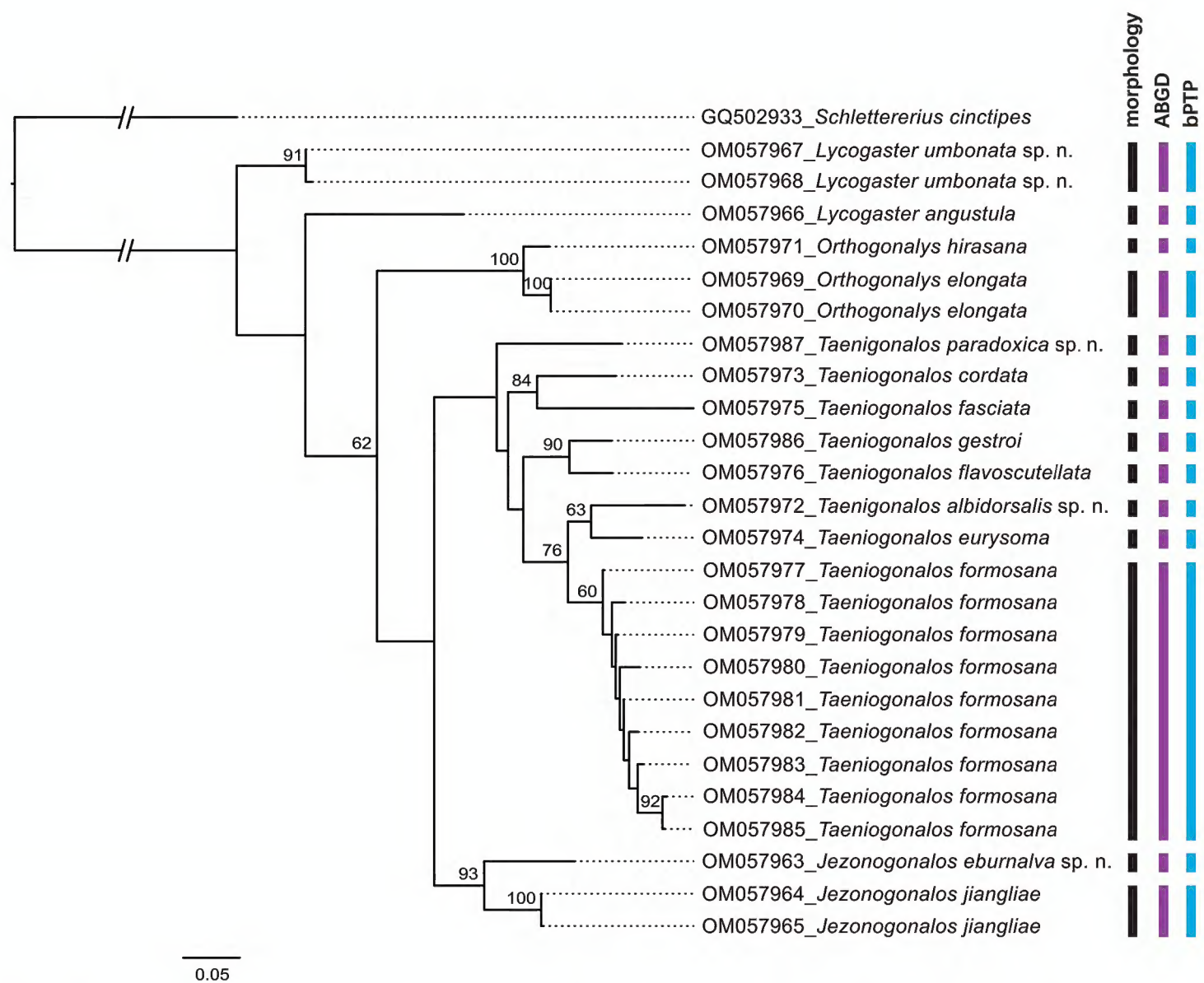


Figure 1. Maximum likelihood tree based on *COI* barcodes and results of species delimitation of three methods, only values > 50 for bootstrap are labeled.

Species treatment

Jezonogonalos Tsuneki, 1991

Figs 2–3

Jezonogonalos Tsuneki, 1991: 32, 2003: 4; Carmean and Kimsey 1998: 70; Chen et al. 2014: 22–44 (diagnosis, key). Type species: *Jezonogonalos marujamae* Tsuneki, 1991 [= *J. marujamae* Tsuneki, 1991], by monotypy. Synonymized with *Pseudogonalos* Schulz, 1906, by Lelej (1995) and re-instated by Chen et al. (2014).

Diagnosis. Length of body 6.2–12.0 mm; antenna black and with 23–27 segments; area above supra-antennal elevations flat, more or less punctate, without protuberance between elevations right after inner side of supra-antennal elevations flat, smooth and black; tyloids of male antenna present on 10th–16th segments, short and nearly circular or elliptical; occipital carina widened medio-dorsally; apical segment of labial palp widened and obtuse, more or less triangular; vertex normal, at most with slight median depression dorsally; mandibles wide in anterior view and sublaterally attached to head; metanotum strongly convex and finely sculptured medially; anterior propodeal sulcus crenulate and medially

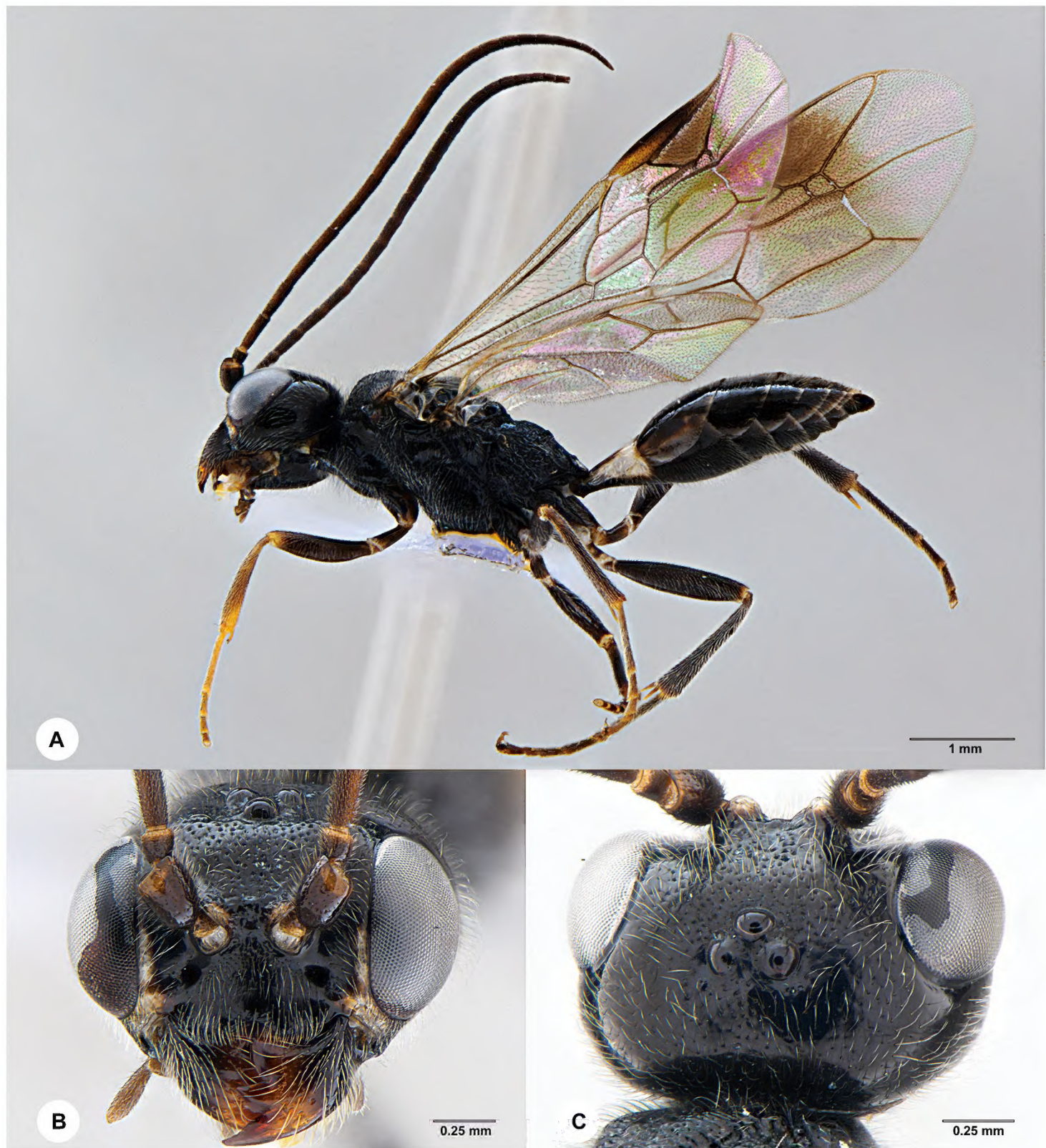


Figure 2. *Jezonogonalos eburnalva* Zhang & Chen, sp. nov., holotype, male (En-419020) **A** habitus, lateral aspect **B** head, anterior aspect **C** head, dorsal aspect.

widened; posterior propodeal carina curved and distinctly protruding and more or less separated from foramen medio-dorsally; fore wing with large dark patch below pterostigma; vein 1-SR of fore wing long; hind trochanter black or ivory; hind tarsus slightly or not modified; second and third sternites of female flat and moderately sclerotized and no protuberances; body rarely with pale pattern, at most malar space, basal segments and margins of metasomal sternites and tergites partly ivory, remainder black (Chen et al. 2014).

Biology. Unknown. Collected in June–November.

Distribution. China, Japan. Before this study, nine species of this genus have been described from China, but none was recorded from Yunnan. We describe here the first species new to science from Yunnan.

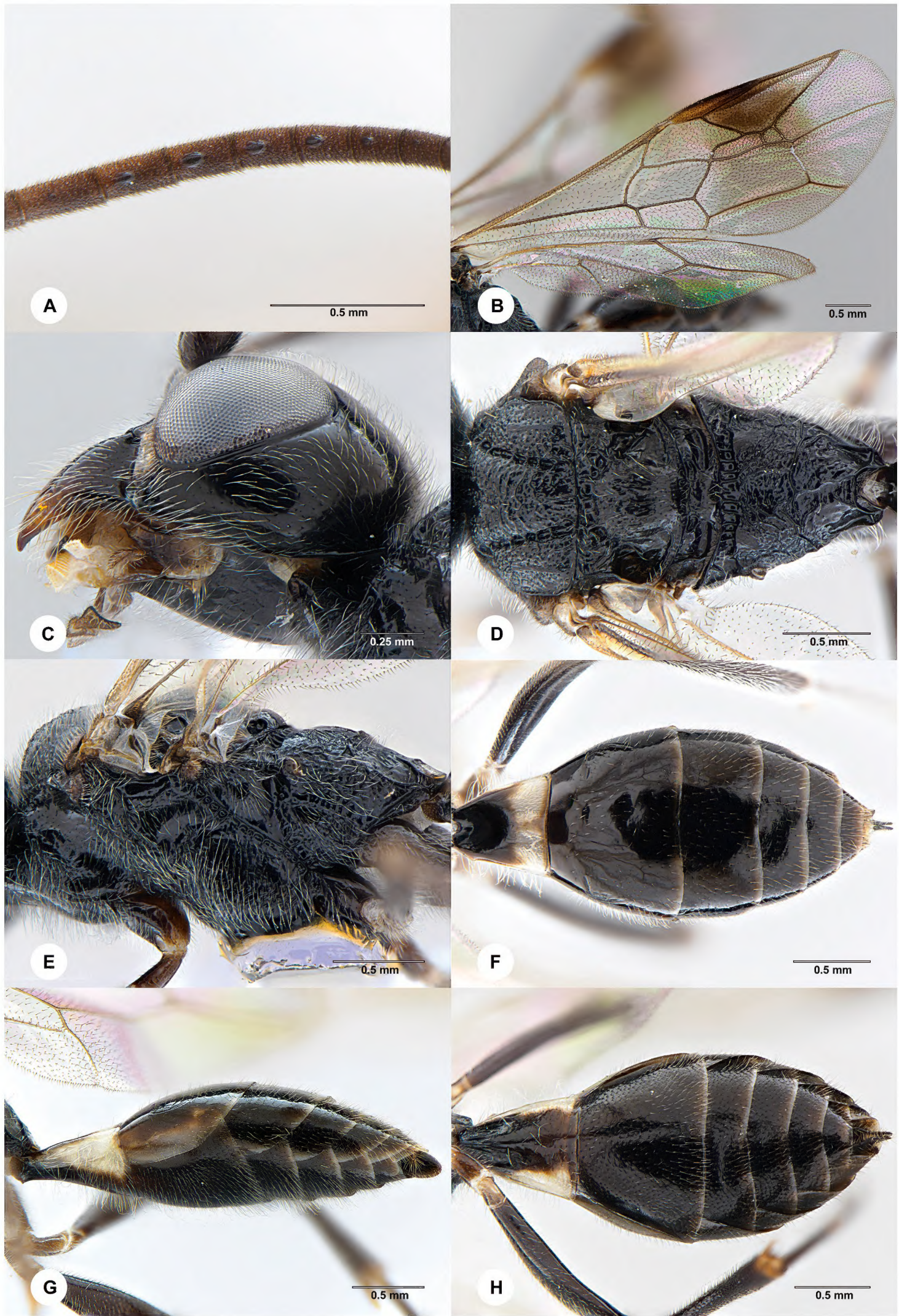


Figure 3. *Jezonogonalos eburnalva* Zhang & Chen, sp. nov., holotype, male (En-419020) **A** tyloids on 10th–16th segments of antenna **B** wings **C** head, lateral aspect **D** mesosoma, dorsal aspect **E** mesosoma, lateral aspect **F** metasoma, dorsal aspect **G** metasoma, lateral aspect **H** metasoma, ventral aspect.

***Jezonogonalos eburnalva* Zhang & Chen, sp. nov.**

<http://zoobank.org/EB7B3D0D-8E14-468E-87F5-06FE870ECAD0>

Figs 2–3

Diagnosis. Occipital carina weakly lamelliform dorsally (Fig. 2C); supra-antennal elevations about 0.2 times as long as scapus and largely ivory dorsally (Fig. 2C); frons densely punctate (Fig. 2C); mandible mainly black, except dark brown base of teeth (Fig. 2B); mesoscutum and propodeum distinctly sculptured; metasoma robust, smooth and largely black except the posterior half of first tergite ivory (Fig. 2A); first tergite approximately as long as its apical width (Fig. 3F); third sternite approximately $0.5 \times$ as long as second sternite (Fig. 3H).

Description. Male. Holotype, length of body 6.2 mm (of fore wing 5.1 mm).

Colour. Black; lower half of inner orbita narrowly ivory and connected to ivory malar space (Fig. 2B); apex of supra-antennal elevation ivory (Fig. 2B); lateral corner of clypeus ivory and connected to ivory malar space; mandibular teeth, palpi dark brown (Fig. 2B); tegulae dark brown; legs mainly black, but tibia and tarsus of fore leg rather brownish (Fig. 2A); apical half of first tergite ivory in dorsal view, nearly all of first tergite ivory in lateral view (Figs 3F, G) and apico-lateral margin of first sternite ivory (Fig. 3H); posterior margin of all other tergites and sternites light ivory (Fig. 3H); pterostigma and posterior half of first submarginal cell to anterior third of marginal cell of fore wing and area below it dark brown to light brown, remainder of wing membrane subhyaline (Fig. 3B).

Head. Antenna with 24 segments (Fig. 2A); tyloids nearly circular on 10th, 15th and 16th segments, oval on 11th–14th segments, $0.1 \times$ as long as segment on 10th, 16th segments and $0.3 \times$ as long as segments on 11th–15th segments (Fig. 3A); frons densely punctate; vertex and temple largely smooth and shiny with sparse and fine punctures; head gradually narrowed behind eyes, eye in dorsal view approximately as long as temple (Fig. 2C); occipital carina narrow lamelliform medio-dorsally and without crenulae; supra-antennal elevations enlarged (about $0.2 \times$ as long as scapus), outer side subvertical and largely smooth except for sparse punctures (Fig. 2C); clypeus slightly concave and thick medio-ventrally.

Mesosoma. Length of mesosoma $1.8 \times$ as long as its height (Fig. 3E); mesopleuron smooth anteriorly and transversely reticulate-rugose posteriorly, transverse mesopleural groove moderately wide and shallow (Fig. 3E); notauli wide, deep and coarsely crenulate; middle lobe of mesoscutum transversely rugose, lateral lobes of mesoscutum mainly finely rugose with a shallow furrow medially (Fig. 3D); scutellar sulcus wide and coarsely crenulate; scutellum shiny, largely smooth with irregular longitudinal rugae, slightly convex medially and anteriorly near level of mesoscutum (Fig. 3E); metanotum medially protruding and obtuse, shiny and largely smooth with sparse fine rugae (Fig. 3D); propodeum reticulate-rugose antero-medially, obliquely rugulose antero-laterally, distinct transversely striate medially, with several longitudinal striae and sparse irregular rugae between large smooth space posteriorly (Fig. 3D); posterior propodeal carina thick lamelliform (foramen approximately $1.4 \times$ as wide as high medially).

Wings. Fore wing: length of vein 1-M $1.6 \times$ as long as vein 1-SR; second submarginal cell $3.1 \times$ as long as third submarginal cell (Fig. 3B).

Metasoma. First tergite approximately as long as its apical width, smooth and with distinct elliptical depression antero-medially, apical half with fine dense longitudinal rugae; second and following tergites shiny and smooth except for sparse superficial punctures (Fig. 3F); sternites rather sparsely finely punctate; second sternite rather flat; third sternite approximately $0.5 \times$ as long as second sternite (Fig. 3H); genitalia extruded (Fig. 3G).

Female. Unknown.

Etymology. Name derived from “*eburnus*” (Latin for “ivory”) and “*alvus*” (Latin for “belly”) because of the large ivory area of the first tergite.

Material examined. **Holotype**, male, CHINA: Yunnan, Mt. Gaoligong, Dulong River, Caihong Bridge, 1496 m, 27°53'51.96"N, 98°20'11.89"E, 2–16.V.2020, Yi Lang leg., MT, SYSBM En-419020 (deposited in SYSBM); GenBank: [OM057963](#).

Distribution. China (Yunnan). Collected at 1496 m.

Comments. This species is similar to *J. jiangliae* but has a relatively short third sternite, more robust first tergite and apical half of tergite ivory, and occipital carina narrow or *J. laeviceps* (shares similar first tergite and second tergite), but it has the mesoscutum and propodeum distinctly sculptured, mandibles dark and occipital carina narrower. The key to species of *Jezonogonalos* published by Tan et al. (2017) could be updated to accommodate *J. eburnalva* by replacing couplet 1 as follows:

- | | |
|----|-----------------------------------------------------------------------------------------------------------------------------------------------------------------------------------------------------------------------------------------------------------------------------------------------------------------------------|
| 1" | First metasomal tergite about as long as its apical width; supra-antennal elevations only apically ivory 1' |
| – | First metasomal tergite 0.6–0.8 times as long as its apical width; at least apical half of supra-antennal elevations yellow or ivory or entirely black 1 |
| 1' | Metasoma of ♂ robust and first tergite with large ivory patch (Figs 3F, G); occipital carina narrow lamelliform medio-dorsally and without crenulae (Fig. 2C); third submarginal cell of fore wing about 0.3 times as long as second submarginal cell (Fig. 3B) <i>J. eburnalva</i> Zhang & Chen, sp. nov. |
| – | Metasoma of ♂ slender and entirely black; occipital carina widened and extensively crenulated dorsally; third submarginal cell of fore wing about 0.4 times as long as second submarginal cell
..... <i>J. jiangliae</i> Chen, van Achterberg, He & Xu, 2014 |

***Lycogaster* Shuckard, 1841**

Figs 4–6

Lycogaster Shuckard, 1841: 121; Weinstein and Austin 1991: 414; Carmean and Kimsey 1998: 61. Type species (by original designation): *Lycogaster pullatus* Shuckard, 1841.

Diagnosis. Body length 5.1–15.0 mm; antenna with 21–24 segments, of female widened medially (but hardly so in *L. angustula*); antenna of male without tyloids; supra-antennal elevations small, without depression dorsally; vertex convex and shiny; mandibular condyli close to level of eyes; apical segment of labial palp widened and



Figure 4. *Lycogaster umbonata* Chen & van Achterberg, sp. nov., holotype, female (En-419021) **A** habitus, lateral aspect **B** head, anterior aspect **C** head, dorsal aspect.

obtuse, more or less triangular; metanotum smooth, shiny and weakly convex; triangular dorso-apical part of hind trochanter separated by an oblique groove; fore trochanter subparallel-sided and distinctly longer than hind trochanter; hind tarsus slightly or not modified; basal half of third metasomal sternite with a posteriorly steep, smooth and complete transverse ledge (may be partly hidden under second sternite and rather low in *L. violaceipennis*); second sternite with pair of small triangular teeth on apical protuberance (but only with pair of lobe-shaped flaps in male of *L. violaceipennis*; with a strong lobe-shaped protuberance medio-apically in female of *L. umbonata* sp. nov.,

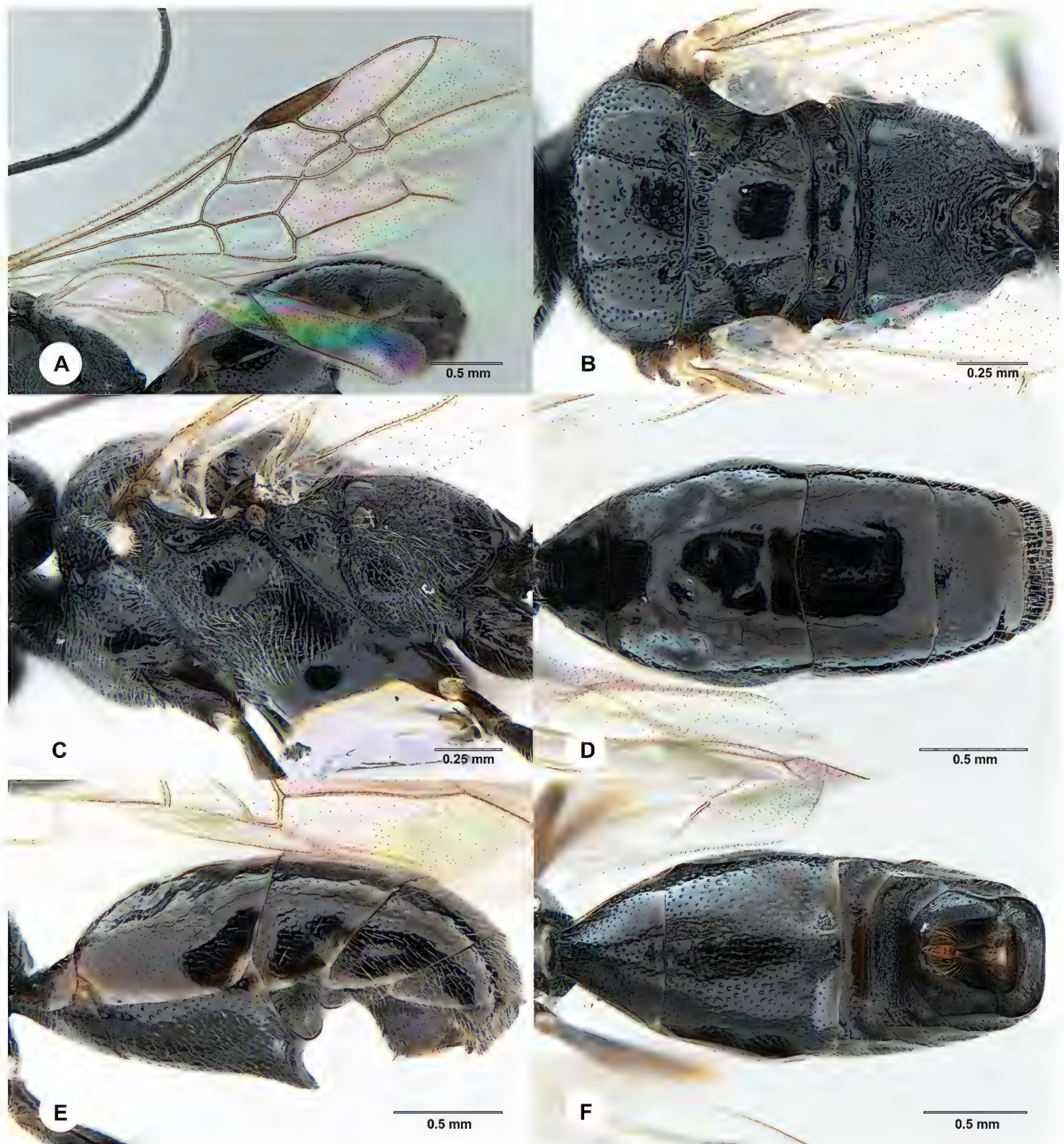


Figure 5. *Lycogaster umbonata* Chen & van Achterberg, sp. nov., holotype, female (En-419021) **A** wings **B** mesosoma, dorsal aspect **C** mesosoma, lateral aspect **D** metasoma, dorsal aspect **E** metasoma, lateral aspect **F** metasoma, ventral aspect.

Figs 4A, 5E, F) and sometimes absent; epipleura of tergites laterally strongly pigmented; fifth sternite of female distinctly emarginate medio-posteriorly.

Biology. In the New World reared as hyperparasitoid of Ichneumonidae in caterpillars of the families Saturniidae and Notodontidae (Carmean and Kimsey 1998).

Distribution. China. Before this study, four species of this genus have been described from China, with only one species recorded from Yunnan. We describe here the second species new to science from Yunnan.

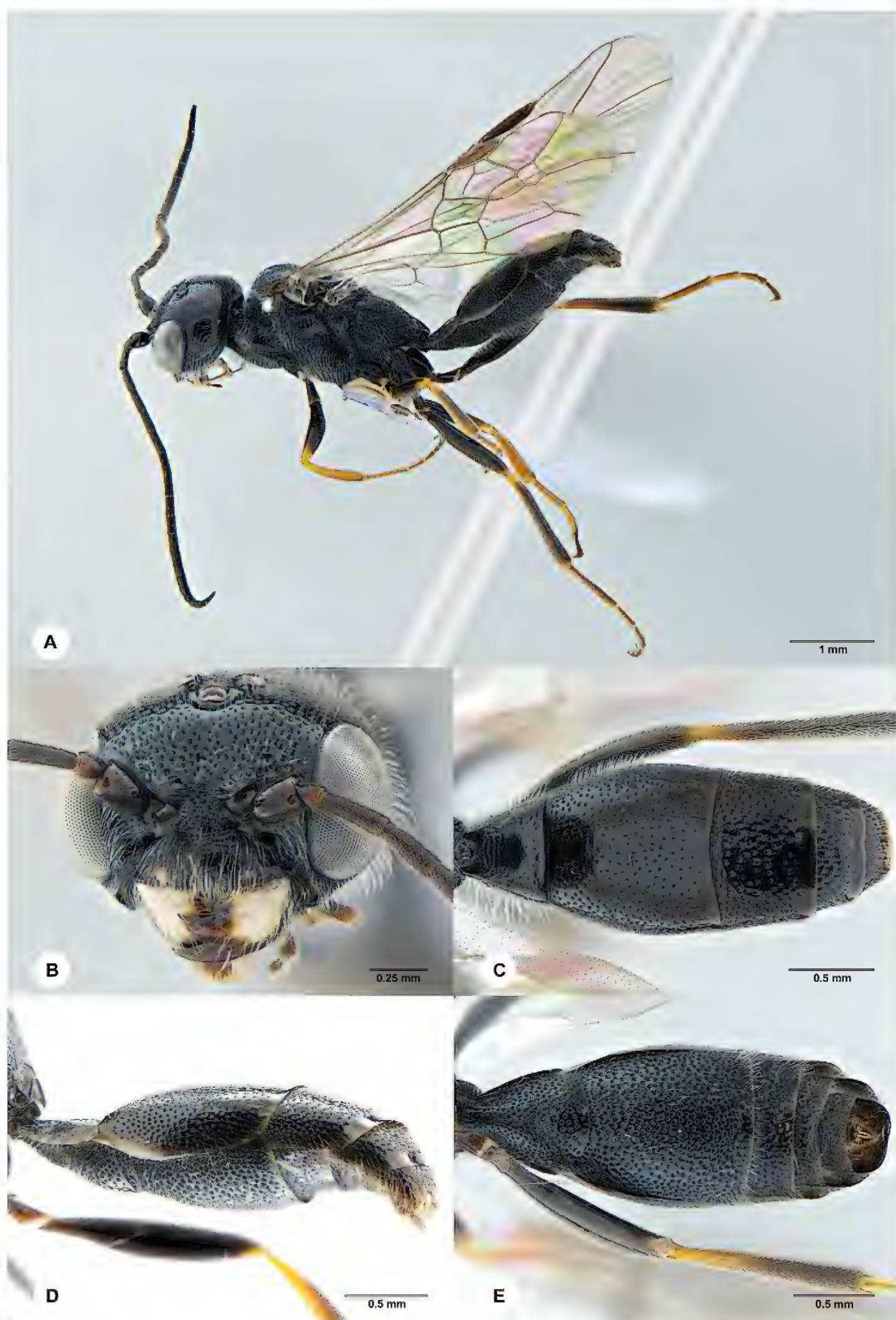


Figure 6. *Lycogaster umbonata* Chen & van Achterberg, sp. nov., paratype, male (En-419022) **A** habitus, lateral aspect **B** head, anterior aspect **C** metasoma, dorsal aspect **D** metasoma, lateral aspect **E** metasoma, ventral aspect.

***Lycogaster umbonata* Chen & van Achterberg, sp. nov.**

<http://zoobank.org/1CA730CA-7C2D-4713-B62D-64BEF9397958>

Figs 4–6

Diagnosis. Antenna elongate and hardly widened medially (Figs 4A, 6A); second sternite of female with a strong lobe-shaped protuberance medio-apically (Fig. 5E); mandibles with ivory patches (Figs 4B, 6B); second tergite of female strongly shiny and with elliptical depressions antero-laterally (Fig. 5D); wing membrane subhyaline and without darkened (Figs 4A, 5A, 6A).

Description. Female. Holotype, length of body 5.1 mm (of fore wing 4.1 mm).

Head. Antenna with 21 segments, elongate and hardly widened medially (Fig. 4A); frons spaced punctate and shiny, with distinct median depression (Fig. 4B); vertex and temple largely smooth and shiny with sparse and fine punctures (Figs 4B, C); head subparallel-sided behind eyes, distinctly narrowed posteriorly and $1.3 \times$ as long as mesoscutum (Fig. 4C); dorsal length of eye approximately as long as temple (Fig. 4C); occipital carina narrow lamelliform and with weak crenulae medio-dorsally (Fig. 4C); supra-antennal elevations hardly developed as a thin rim and smooth, $0.3 \times$ as long as scapus (Fig. 4C); clypeus emarginate and comparatively thin medio-ventrally (Fig. 4B).

Mesosoma. Length of mesosoma $1.8 \times$ as its height (Fig. 5C); mesopleuron below transverse mesopleural groove rugose to punctate anteriorly, largely smooth and shiny posteriorly, above groove similar but rugose anteriorly (Fig. 5C); notauli narrow anteriorly, widened posteriorly and coarsely crenulate; middle lobe of mesoscutum sparsely and rather finely punctate anteriorly, coarsely punctate at posterior end, lateral lobes sparsely and rather finely punctate (Fig. 5B); scutellar sulcus wide, both medially and laterally and coarsely crenulate (Fig. 5B); scutellum largely smooth with sparsely and finely punctate, distinctly shiny, rather flat and anteriorly near level of mesoscutum; metascutellum shiny and smooth medio-posteriorly (Fig. 5B); propodeum largely obliquely rugulose to rugose with smooth interspaces antero-laterally (Fig. 5B); posterior propodeal carina thick lamelliform and distinctly arched, foramen approximately $1.5 \times$ as wide as high medially (Fig. 5B).

Wings. Fore wing: length of vein 1-M $1.8 \times$ as long as vein 1-SR; second submarginal cell $1.4 \times$ as long as third submarginal cell (Fig. 5A).

Metasoma. First tergite $0.5 \times$ as long as its apical width, smooth, with rather distinct elliptical depression medially and basal half with several distinct coarse transverse rugae medially (Fig. 5D); second tergite with elliptical depressions antero-laterally; second-fifth tergites largely smooth with sparse fine punctures (Fig. 5D); sternites sparsely and finely punctate (Fig. 5F); second sternite strongly convex in lateral view, with a strong lobe-shaped protuberance medio-apically (Fig. 5E); third sternite about $0.2 \times$ as long as second sternite, with distinct ledge (Fig. 5F); hypopygium truncate apically (Fig. 5F).

Colour. Black; mandibular teeth and palpi dark brown; anterior-basal part of mandible ivory (Fig. 4B); distal of fumer, tibia, tarsus and claw yellow to brownish (Fig. 4A); pterostigma dark brown; wing membrane subhyaline and without darkened (Fig. 4A).

Male. Paratype, length of body 5.9 mm, of fore wing 4.5 mm; antenna with 21 segments and without tyloids (Fig. 6A); vertex densely and coarsely punctate; sculp-

ture of mesosoma coarser than that in female (Fig. 6B); second tergite with a round depression antero-medially; second-fifth tergites and sternites densely and rather fine punctate, except sparsely and coarsely punctate in big round area of third tergite medially (Figs 6C–E); genitalia extruded (Fig. 6D); ivory part of mandible larger than that of female; clypeus with ivory patches (Fig. 6B); large part of hind tibia, hind tarsus and hind claw brown (Fig. 6A), not like that in female.

Etymology. Named after the strong lobe-shaped protuberance of female second sternite: from “*umbo*” (Latin for “rounded protuberance”).

Material examined. *Holotype*, female, CHINA: Yunnan, Baoshan City, Longyang Dist., 2390 m, 25°17'57.26"N, 98°46'11.35"E, 15–30.IX.2020, Lang Yi leg., MT, SYSBM En-419021 (deposited in SYSBM); GenBank: [OM057968](#). *Paratype*, 1 male, CHINA: Yunnan, Baoshan City, Longyang Dist., 2390 m, 25°17'57.26"N, 98°46'11.35"E, 30.VII–15.VIII.2020, Lang Yi leg., MT, SYSBM En-419022 (SYSBM); GenBank: [OM057967](#).

Distribution. China (Yunnan). Collected at 2390 m.

The key to Chinese species of *Lycogaster* published by Chen et al. (2014) could be updated to accommodate *L. umbonata* by replacing couplet 2 as follows:

- 2 Female antenna elongate and hardly widened medially (Fig. 4A); second tergite smooth and strongly shiny (Fig. 5D); medial third of fore wing subhyaline (Figs 4A, 5A, 6A) or slightly darkened.....**2'**
- Female antenna less elongate and distinctly widened medially; second tergite punctate and moderately shiny; medial third of fore wing largely dark brown**3**
- 2' Medio-apical protuberance of second sternite with pair of small submedial acute teeth close to each other; posterior end of middle lobe of mesoscutum rugose ***L. angustula* Chen, van Achterberg, He & Xu**
- Medio-apical protuberance of second sternite obtuse, lamelliform and convex medio-apically, without small submedial acute teeth (Fig. 5E); posterior end of middle lobe of mesoscutum largely smooth with sparse fine punctures (Fig. 5B) ***L. umbonata* Chen & van Achterberg, sp. nov.**

***Taeniogonalos* Schulz, 1906**

Figs 7–10

Taeniogonalos Schulz, 1906: 212; Weinstein and Austin 1991: 416; Tsuneki 1991: 59; Carmean and Kimsey 1998: 65. Type species (by monotypy): *Trigonalys maculata* Smith, 1851.

Labidogonalos Schulz, 1906: 207; Weinstein and Austin 1991: 414; Carmean and Kimsey 1998: 65. Type species (by monotypy): *Trigonalys ornata* Smith, 1851.

Poecilogonalos Schulz, 1906: 212; Marshakov 1981: 105; Tsuneki 1991: 46; Weinstein and Austin 1991: 422; Tsuneki 1991: 46; Lelej 1995: 14. Type species (by monotypy): *Trigonalys thwaitesii* Westwood, 1874. Synonymized by Carmean and Kimsey 1998.

- Nanogonalos* Schulz, 1906: 211; Teranishi 1929: 150; Marshakov 1981: 107; Tsuneki 1991: 56; Weinstein and Austin 1991: 421. Synonymized by Carmean and Kimsey 1998. Type species (by monotypy): *Nanogonalos enderleini* De Santis, 1980.
- Ischnogonalos* Schulz, 1907: 11; 1908: 33; Bischoff 1933: 482, 1938: 11; Weinstein and Austin 1991: 413; Carmean and Kimsey 1998: 65. Type species (by monotypy): *Trigonalys dubia* Magretti, 1997.
- Lycogastroides* Strand, 1912: 129; Weinstein and Austin 1991: 413. Type species (by original designation): *Lycogastroides gracilicornis* Strand, 1912. Synonymized by Carmean and Kimsey 1998.
- Lycogonalos* Bischoff, 1913: 155; Weinstein and Austin 1991: 415. Type species (by original designation): *Lycogonalos flavicincta* Bischoff, 1913. Synonymized by Carmean and Kimsey 1998.
- Taiwanogonalos* Tsuneki, 1991: 35. Type species (by original designation): *Taiwanogonalos alishana* Tsuneki, 1991. Synonymized by Carmean and Kimsey 1998.

Diagnosis. Body length 4.3–13.0 mm; antenna with 21–26 segments, without pale band and slender medially, of male with linear tyloids (= elevated elongate areas) on 10th–16th antennal segments; supra-antennal elevations smooth or punctate, without depression dorsally, remain far separated from each other medially and without horizontal “shelf” between antennal bases; temple usually punctate or reticulate-punctate and moderately shiny; occipital carina ending at hypostomal carina at level of mandibular base; vertex flattened, without median depression dorsally; apical segment of labial palp widened and obtuse, more or less triangular; mandibles wide in anterior view and sublaterally attached to head; mesoscutum and scutellum distinctly punctate or rugose; metanotum at least partly convex latero-dorsally and often sculptured; vein 1-SR of fore wing medium-sized to long; fore wing often with subapical dark patch or large part of fore wing dark brown; triangular dorso-apical part of hind trochanter separated by an oblique groove; fore trochanter subparallel-sided and distinctly longer than hind trochanter; hind tarsus slightly or not modified; propodeal foramen more or less arched dorsally and often with a lamelliform carina; second sternite convex in lateral view (but less so in males), strongly sclerotized and frequently densely punctate, sometimes with a medio-posterior elevation but without pair of small teeth; basal half of third sternite flat, without a distinct ledge anteriorly; hypopygium of female pointing anteriorly toward second sternite or straight down or pointing posteriad; body variable, often moderately robust.

Biology. Reared as hyperparasitoid of parasitoid wasps (Ichneumonidae and Braconidae) and parasitoid flies (Tachinidae) in lepidopteran or sawfly caterpillars, but some species are primary parasitoids of Pergid sawflies in Australia (Raff 1934; Carne 1969; He and Chen 1986; Weinstein and Austin 1995; Carmean and Kimsey 1998; He 2004).

Distribution. China, Russia, Mongolia, India, Sri Lanka, Thailand, Laos, Papua New Guinea, Myanmar, Malaysia, Indonesia, Japan. Before this study, 20 species of this genus have been described from China, with eight recorded from Yunnan. We describe here two species new to science from Yunnan. Until now, four species in this genus were only found in Yunnan.

***Taeniogonalos albidorsalis* Zhang & Chen, sp. nov.**

<http://zoobank.org/D9CA17E6-06DF-464B-9F17-9788D8154A55>

Figs 7–8

Diagnosis. Supra-antennal elevations approximately $0.4 \times$ as long as scapus and their outer side oblique (Fig. 7C); occipital carina narrow, non-lamelliform, smooth (Fig. 7C); head anteriorly and posteriorly black, pronotum white dorsally, tegulae dark brown (Figs 7B, C, 8C, D); vertex largely sparsely and finely punctate, with rather coarse punctures and slightly rugose media-posteriorly (Fig. 7C); mesoscutum coarsely sculptured in dorsal view (Fig. 8C); notauli wide and crenulate (Fig. 8C); scutellum coarsely rugose, convex laterally and shallowly concave medially (Fig. 8C); metanotum slightly convex, rugose (Fig. 8C); posterior propodeal carina distinctly arched, narrow lamelliform, foramen comparatively narrow (Fig. 8D); posterior margin of tergites with brownish stripes (Fig. 8E); first sternite dark brown posteriorly (Fig. 8F); second sternite slightly convex (Fig. 8F); third sternite without depression (Fig. 8F).

Description. Female. Holotype, length of body 7.1 mm (of fore wing 5.9 mm).

Head. Antenna with 22 segments; frons reticulate-punctate (Fig. 7B); vertex largely sparsely and finely punctate, with rather coarse punctures and slightly rugose media-posteriorly (Fig. 7C); temple largely smooth with few punctures at orbita (Fig. 8B); head gradually narrowed behind eyes, eye in dorsal view $0.8 \times$ as long as temple (Fig. 7C); occipital carina narrow, non-lamelliform, smooth (Fig. 7C); supra-antennal elevations smooth with outer side oblique, $0.4 \times$ as long as scapus (Fig. 7C); clypeus slightly concave and thick medio-ventrally (Fig. 7B).

Mesosoma. Length of mesosoma $1.5 \times$ as long as its height (Fig. 8D); transverse mesopleural groove narrow, crenulate; mesopleuron above transverse mesopleural groove coarsely rugose anteriorly and smooth posteriorly, below groove largely punctate (Fig. 8D); notauli wide, deep and coarsely crenulate; middle lobe of mesoscutum smooth anteriorly, otherwise transversely punctate-rugose, lateral lobes largely punctate-rugose (Fig. 8C); scutellar sulcus complete, moderately narrow and crenulate; scutellum coarsely rugose and shallowly concave medially, anteriorly distinctly above level of mesoscutum; metanotum slightly convex, rugose (Fig. 8C); propodeum punctate-rugose (Fig. 8C); posterior propodeal carina distinctly arched, narrow lamelliform, foramen approximately $1.3 \times$ as wide as high medially.

Wings. Fore wing: vein 1-M $1.4 \times$ as long as vein 1-SR; second submarginal cell $1.3 \times$ as long as third submarginal cell (Fig. 8A).

Metasoma. First tergite $0.4 \times$ as long as its apical width, smooth and with shallow but wide depression medially (Fig. 8E); second tergite largely smooth and finely punctate laterally; following tergites moderately punctate (Fig. 8E); first sternite sparse punctate and concave laterally; second sternite slightly convex, densely and finely punctate; lateral sides from third to fifth sternites and anterior of fourth sternite without punctation, otherwise moderately punctate (Fig. 8F).

Colour. Black; antenna largely brownish (except apex and scapus) (Fig. 7A); outer orbita with pale yellow stripes, inner orbita with brownish short strips, malar space



Figure 7. *Taeniogonalos albidorsalis* Zhang & Chen, sp. nov., holotype, female (En-419023) **A** habitus, lateral aspect **B** head, anterior aspect **C** head, dorsal aspect.

yellow brown patches; lateral corner of clypeus brownish; mandibles brown to dark brown, with basal pale patches (Figs 7B, 8B); pair of ivory triangular patches on middle lobe of mesoscutum anterior-laterally, pair of ivory to brownish patches on antero-lateral margin of scutellum, metanotum white with brownish patches (Fig. 8C); palpi brown (Fig. 8B), tegulae dark brown (Fig. 8D); about posteriorly half of first tergite ivory; margin of other tergites with ivory to brownish stripes (Fig. 8E); fifth tergite with two elongated ivory patches media-posteriorly (Fig. 8E); first sternite dark brown posteriorly (Fig. 8F); coxa and trochanter of hind leg mainly white; tarsi and tibia of fore leg mainly yellow to brownish (Fig. 7A); pterostigma dark brown; apical half of



Figure 8. *Taeniogonalos albidorsalis* Zhang & Chen, sp. nov., holotype, female (En-419023) **A** wings **B** head, lateral aspect **C** mesosoma, dorsal aspect **D** mesosoma, lateral aspect **E** metasoma, dorsal aspect **F** metasoma, ventral aspect.

marginal cell of fore wing largely infusate as area below it, remainder of wing membrane subhyaline (Figs 7A, 8A).

Male. Unknown.

Etymology. The specific epithet originates from “*albus*” (Latin for “white”) and “*dorsalis*” (Latin for “dorsal”) with reference to the white dorsal part of the pronotum.

Material examined. *Holotype* CHINA: ♀; Yunnan, Mt. Gaoligong, Dulong River, Qinlangdang Management and Protection Station, 1181 m, 27°41'6.73"N,

98°16'25.64"E; 15.V–15.VI.2020, Lang Yi leg., MT, SYSBM En-419023 (deposited in SYSBM); GenBank: [OM057972](#).

Distribution. China (Yunnan). Collected at 1181 m.

Comments. This species is close to *T. eury soma* and it would run to that taxon (couplet 17) in the revised key of Tan et al. (2017), but can be distinguished by having largely brownish antenna, dorsally white pronotum, pale and more elongate fore tibia, less sculptured vertex, and second sternite without ivory stripe. Part of key to Chinese species of the genus *Taeniogonalos* Schulz was revised to include *T. eury soma* Chen & van Achterberg, 2020.

- 17 Second metasomal sternite of female less convex medially and in lateral view its ventral border gradually sloping posteriorly, strongly shiny medially and third sternite smooth anteriorly or nearly so; second sternite of male evenly slightly convex medio-posteriorly; vertex often strongly shiny **18**
- Second sternite of female strongly convex medially and in lateral view its ventral border distinctly sloping posteriorly, moderately shiny medially and third sternite distinctly punctate anteriorly; second sternite of male slightly flattened medio-posteriorly; vertex moderately shiny **20**
- 18 Propodeum comparatively narrow, almost triangular in dorsal view (especially male, less so in female) and with nearly straight lateral margins; outer orbita black; supra-antennal elevations about half as long as scapus *T. alticola* (Tsuneki, 1991)
- Propodeum somewhat wider, more oval in dorsal view and lateral margins curved; outer orbita with pale stripes; supra-antennal elevations smaller (about 0.2 times as long as scapus) **19**
- 19 Antenna mainly blackish; pronotum dorsally black; fore tibia comparatively dark and short; metasomal segments rather wide; second sternite with ivory stripe *T. eury soma* Chen & van Achterberg, 2020
- Antenna largely brownish (Fig. 7A); pronotum dorsally white (Fig. 8C); fore tibia comparatively pale and more elongate (Fig. 7A); vertex less sculptured (Fig. 7C); metasomal segments comparatively elongate (Fig. 8E); second sternite without ivory stripe *T. albidorsalis* Zhang & Chen, sp. nov.
- 20 Vertex with elongate brownish patches; third and fourth metasomal tergites very coarsely punctate; metanotum with a pair of yellow spots medially; third sternite coarsely and densely punctate medio-posteriorly (male) or latero-posteriorly (female) in front of membranous border; [propodeal foramen comparatively wide and less arched]. *T. formosana* (Bischoff, 1913)
- Vertex entirely black or rarely with small brownish patches; third and fourth metasomal tergites usually superficially punctate, rarely nearly as coarse as in *T. formosana*; metanotum black medially and at most with a pair of lateral yellow spots; third sternite usually more spaced and finer punctate posteriorly *T. taihorina* (Bischoff, 1914)

***Taeniogonalos paradoxica* Zhang & Chen, sp. nov.**

<http://zoobank.org/E20EB99B-85AB-408D-AAF9-A46CB9481F01>

Figs 9–10

Diagnosis. Supra-antennal elevations $0.5 \times$ as long as scapus and outer side strongly steep (angle about 70°), upper half thickened and backward, parallel-sided in anterior view, area between elevations with a small protuberance (Figs 9B, C); tyloids of male antenna linear (Fig. 10A); occipital carina widened, lamelliform and smooth (Fig. 9C); supra-antennal elevations largely yellow; head with brownish-yellow oblique patches postero-laterally (Fig. 9C); vertex largely coarsely punctate with transversely rugose and becoming sparsely punctate posteriorly (Fig. 9C); mesoscutum coarsely punctate-rugose in dorsal view, with pair of large triangular yellow patches on middle lobe and pair of large oblong yellow patches on scutellum axilla (Fig. 10D); notauli narrow anteriorly, widened posteriorly and coarsely crenulate (Fig. 10D); scutellum coarsely reticulate-punctate and shallow-slightly concave medially, with pair of small brown-yellow patches (Fig. 10D); metanotum slightly convex, rugose, with four elliptical yellow patches (Fig. 10D); posterior propodeal carina distinctly arched, narrow lamelliform, foramen comparatively wide (Fig. 10D); first tergite with yellow stripe posteriorly; second tergite widely yellow posteriorly, third tergite with weak and slim yellow patches medio-posteriorly; fourth-sixth tergites with large yellow patches (Fig. 10F); first and second sternites with wavy yellow stripe posteriorly; third and fourth sternites with small yellow patches postero-laterally (Fig. 10G); second sternite slightly concave medio-anteriorly (Fig. 9A); third sternite without depression (Fig. 10G).

Description. Female. Holotype, length of body 8.6 mm (of fore wing 7.1 mm).

Head. Antenna with 23 segments; tyloids linear, $0.6 \times$ as long as antennal segment on 11th–13th segments, about half as long on 14th segment, $0.3 \times$ as long on 15th segment and $0.2 \times$ as long on 10th segment (Fig. 10A); frons densely and coarsely punctate with rugae near clypeus (Fig. 9B); vertex largely coarsely punctate with transversely rugae and becoming sparsely punctate posteriorly (Fig. 9C); temple largely smooth with few punctures near orbita (Fig. 10C); head gradually narrowed behind eyes, eye in dorsal view $0.8 \times$ as long as temple (Fig. 9C); occipital carina widened, lamelliform and smooth (Fig. 9C); supra-antennal elevations smooth, outer side very steep (angle about 70°), upper half thickened and backward, parallel-sided in anterior view, $0.5 \times$ as long as scapus, with a small protuberance between them (Fig. 9B, C); clypeus slightly concave and thick medio-ventrally (Fig. 9B).

Mesosoma. Length of mesosoma $1.7 \times$ as long as its height (Fig. 10E); transverse mesopleural groove narrow, crenulate; mesopleuron above transverse mesopleural groove reticulate-punctate anteriorly and coarsely punctate posteriorly, below groove rugulose-punctate anteriorly and smooth posteriorly (Fig. 10E); notauli narrow anteriorly, widened posteriorly and coarsely crenulate; middle lobe of mesoscutum coarsely transversely punctate-rugose anteriorly and reticulate-punctate posteriorly, lateral lobes largely punctate with longitudinal rugae (Fig. 10D); scutellar sulcus complete, moderately narrow and crenulate; scutellum coarsely reticulate-punctate and slightly concave medially, anteriorly protruding above level of mesoscutum; metanotum slightly convex, rugose (Fig. 10D); propodeum punctate-rugose (Fig. 10D); posterior propodeal carina distinctly arched, narrow lamelliform, foramen approximately $1.5 \times$ as wide as high medially.



Figure 9. *Taeniogonalos paradoxa* Zhang & Chen, sp. nov., holotype, male (En-419024) **A** habitus, lateral aspect **B** head, anterior aspect **C** head, dorsal aspect.

Wings. Fore wing: vein 1-M $1.2 \times$ as long as vein 1-SR; second submarginal cell $1.1 \times$ as long as third submarginal cell (Fig. 10B).

Metasoma. First tergite $0.6 \times$ as long as its apical width, smooth and with shallow but wide depression medially (Fig. 10F); following tergites densely and coarsely punctate (Fig. 10F); first sternite sparse punctate and concave laterally; following sternites densely punctate (Fig. 10G); second sternite slightly concave medio-anteriorly, rather flat medio-posteriorly and slightly depressed near middle of posterior margin (Figs 9A, 10G).

Colour. Black; apical half of antenna and part of scapus dark brown; remainder of antenna mainly yellow; orbita yellow, narrow but widened near antennal sockets; supra-antennal elevations largely yellow; clypeus with pair of yellow patches; lateral

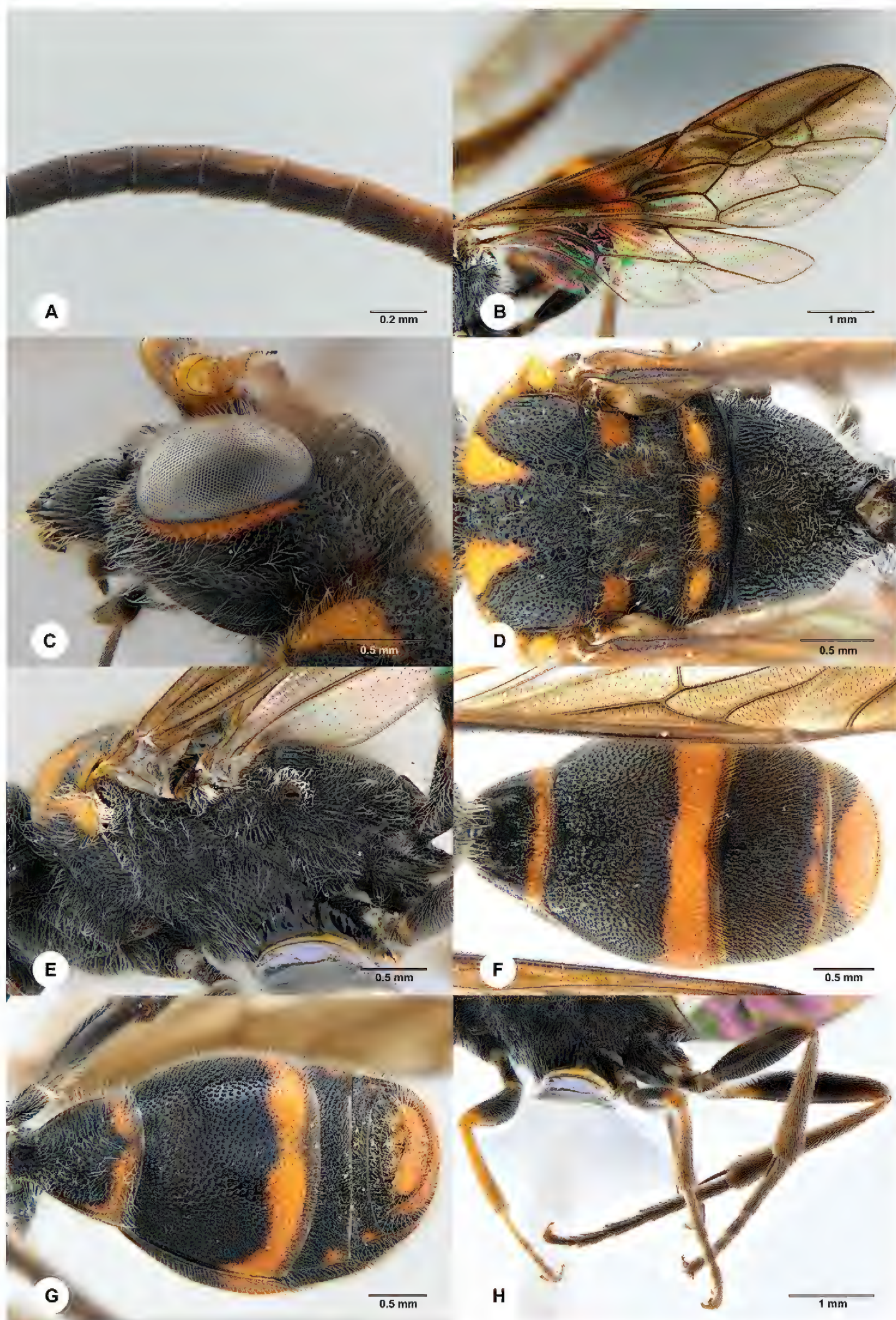


Figure 10. *Taeniogonalos paradoxica* Zhang & Chen, sp. nov., holotype, male (En-419024) **A** tyloids on 10th–16th segments of antenna **B** wings **C** head, lateral aspect **D** mesosoma, dorsal aspect **E** mesosoma, lateral aspect **F** metasoma, dorsal aspect **G** metasoma, ventral aspect **H** legs, ventral aspect.

corner of clypeus dark brown; mandible teeth dark brown to dark (Fig. 9B); head with brownish-yellow oblique patches postero-laterally (Fig. 9C); pronotum yellow dorsally (Fig. 10D); middle lobe of mesoscutum with pair of large triangular yellow patches antero-laterally; scutellum axilla with pair of large oblong yellow patches; scutellum with pair of small brown-yellow patches media-laterally; metanotum with four elliptical yellow patches (Fig. 10D); palpi dark brown (Fig. 10C); tegulae brown (Fig. 10D); first tergite with yellow stripe posteriorly; second tergite widely yellow posteriorly, third tergite with weak and slim yellow patches media-posteriorly; fourth-sixth tergites with large yellow patches (Fig. 10F); first and second sternites with wavy yellow stripe posteriorly; third and fourth sternites with small yellow patches postero-laterally (Fig. 10G); apex of fore and middle femora yellow; tibiae and basal half of tarsi of fore leg largely yellow; remainder of tibiae and tarsi dark brown (Fig. 10H); pterostigma yellow brown; anterior half of fore wing dark brown; remainder of wing subhyaline (Fig. 10B).

Male. Unknown.

Etymology. Name after the unusual supra-antennal elevations: from “*paradoxus*” (Latin for “strange, contrary to expectation”).

Material examined. *Holotype*, female, CHINA: Yunnan, Diqing Tibetan Autonomous Prefecture, Shangri-La City, Jiantang town, apple orchard, 2639 m, 27°31'36"N, 100°5'32"E, 20.IX.2020, Huayan Chen leg., YPT, SYSBM En-419024 (deposited in SYSBM); GenBank: [OM057987](#).

Distribution. China (Yunnan). Collected at 2639 m.

The key to species of *Taeniogonalos* published by Chen et al. (2014) could be updated to accommodate *T. paradoxica* by replacing couplet 12 as follows:

- | | |
|-----|---------------------------------------------------------------------------------------------------------------------------------------------------------------------------------------------------------------------------------------------------------------------------------------------------------------------------------------------------------------------------------------------------------------------------------------------|
| 12 | Protuberance of third sternite of ♀ subtruncate medio-apically; pronotum, metanotum medially and head of ♀ posteriorly with pale pattern; hind tibia black or dark brown; outer sides of supra-antennal elevations oblique..... 12' |
| – | Protuberance of third sternite of ♀ acutely protruding medio-apically; metanotum, apex of supra-antennal elevations and head posteriorly in dorsal view black; hind tibia brown; outer side of supra-antennal elevations subvertical..... 13 |
| 12' | Pronotum black dorsally; metanotum ivory medially; apex of supra-antennal elevations pale yellowish and remainder black; head of ♀ posteriorly with pair of ivory patches in dorsal view (black in ♂); hind tibia black; outer side of supra-antennal elevations oblique; metanotum with pair of yellowish patches..
..... <i>T. subtruncata</i> Chen, van Achterberg, He & Xu, 2014 |
| – | Pronotum yellow dorsally (Fig. 10D); supra-antennal elevations largely yellow (Figs 9B, C); head of ♂ posteriorly with pair of brownish-yellow oblique patches in dorsal view (Fig. 9C); hind tibia dark brown (Fig. 10H); outer side of supra-antennal elevations strongly steep (angle about 70°; Fig. 9C); metanotum with four elliptical yellow patches (Fig. 10D).....
..... <i>T. paradoxica</i> Zhang & Chen, sp. nov. |

Discussion

Recently, DAN barcode-based methods have become increasingly popular for the identification of parasitoids (Talamas et al. 2019; Chen et al. 2020b; Mo et al. 2021; Liu et al. 2021; Olmi et al. 2022). These methods are especially powerful in providing evidence of species boundaries that supplement morphological identifications as well as confirmation of female-male association for species with sexual dimorphism (Liu et al. 2021; Olmi et al. 2022). Although we only provide *COI* sequences for 14 species in this study, the results indicate that the use of DNA barcoding for the identification of Trygonalyidae species is also powerful. The intraspecific pairwise distances are generally less than 3%, while the interspecific pairwise distances are higher than 5% (Suppl. material 2: Table S2; Suppl. material 3: Table S3). *Lycogaster* species usually show evident sexual dimorphism in metasomal structures, as can be seen in *Lycogaster umbonata* that we describe here. However, the *COI* sequences from the female and male specimens of *Lycogaster umbonata* are more than 99% identical, allowing us to confirm their association. In short, the results of our study demonstrate that molecular data are useful to enhance species delimitation and the female-male association of the same species in Trygonalyidae.

The diversity of Trigonalyidae in the East Palaearctic and Northeast Oriental regions is much higher than in other regions, e.g., from the West Palaearctic region only one species is known. The discovery of four new species from SW China shows that the Chinese fauna remains undersampled as already noted by Chen et al. (2014). The relationships of the new species are all among other species occurring in the same region but at least partly at lower altitudes. The adaptation to high altitudes may be the major driver of the evolution among Trigonalyidae and the more or less isolated mountains are an extra impetus to the radiation of species in both regions.

Acknowledgements

Thanks to Yu-ye Tong (Sun Yat-sen University) for his help in taking some of the images. This research was supported by the Wencheng County's Second Phase of Innovation and Entrepreneurship Seed Fund in 2019 (2019NKY09), the Biodiversity Survey and Assessment Project of the Ministry of Ecology and Environment, China (2019HJ2096001006), and National Animal Collection Resource Center, China.

References

- Carmean D (1991) Biology of the Trigonalyidae (Hymenoptera), with notes on the vespine parasitoid *Bareogonalos canadensis*. New Zealand Journal of Zoology 18: 209–214. <https://doi.org/10.1080/03014223.1991.10757968>

- Carmean D, Kimsey L (1998) Phylogenetic revision of the parasitoid wasp family Trigonalidae (Hymenoptera). *Systematic Entomology* 23: 35–76. <https://doi.org/10.1046/j.1365-3113.1998.00042.x>
- Carne PB (1969) On the population dynamics of the *Eucalyptus*-defoliating sawfly *Perga affinis affinis* Kirby (Hymenoptera). *Australian Journal of Zoology* 17: 113–141. <https://doi.org/10.1071/ZO9690113>
- Chen H-Y, Hong C-D, van Achterberg C, Pang H (2020a) New species and new records of Trigonalidae (Hymenoptera) from Tibet, China. *ZooKeys* 918: 83–98. <https://doi.org/10.3897/zookeys.918.49729>
- Chen H, Talamas EJ, Bon M-C, Moore MR (2020b) *Gryon ancilla* Kozlov & Lê (Hymenoptera: Scelionidae): host association, expanded distribution, redescription and a new synonymy. *Biodiversity Data Journal* 8: e47687. <https://doi.org/10.3897/BDJ.8.e47687>
- Chen H-Y, van Achterberg C, He J-H, Xu Z-F (2014) A revision of the Chinese Trigonalidae (Hymenoptera, Trigonoidea). *ZooKeys* 385: 1–207. <https://doi.org/10.3897/zookeys.385.6560>
- Clausen CP (1940) *Entomophagous Insects*. McGraw-Hill, New York.
- Folmer O, Black M, Hoeh W, Lutz R, Vrijenhoek R (1994) DNA primers for amplification of mitochondrial cytochrome c oxidase subunit I from diverse metazoan invertebrates. *Molecular Marine Biology and Biotechnology* 3: 294–299.
- He J-H (2004) *Hymenopteran Insect Fauna of Zhejiang*. Science Press, Beijing. [in Chinese]
- He J-H, Chen H-L (1986) *Poecilognathos flavoscutellata* Chen (Hymenoptera: Trigonalidae), an epiparasite of the *Locastra muscosalis* Walker (Lepidoptera: Pyralidae). *Acta Agriculturae Universitatis Zhejiangensis* 12(2): 231–232. [in Chinese]
- Katoh K, Standley DM (2013) MAFFT multiple sequence alignment software version 7: Improvements in performance and usability. *Molecular Biology and Evolution* 30: 772–780. <https://doi.org/10.1093/molbev/mst010>
- Kim C-J, Tan J-L, Lee B-W, Oh S-H, Choi M-B (2020). Discovery of a trigonalid wasp, *Bareognathos xibeidai* (Hymenoptera: Trigonalidae), reared from nests of *Vespula koreensis koreensis* (Hymenoptera: Vespidae) in South Korea. *Journal of Asia-Pacific Biodiversity* 13: 380–383. <https://doi.org/10.1016/j.japb.2020.06.006>
- Kumar S, Stecher G, Tamura K (2016). MEGA7: Molecular evolutionary genetics analysis version 7.0 for bigger datasets. *Molecular Biology and Evolution* 33: 1870–1874. <https://doi.org/10.1093/molbev/msw054>
- Lelej AS (2019) Family Trigonalidae (Trigonalidae) – Trigonalid wasps. In: Belokobylskij SA, Samartsev KG, Il'inskaya AS (Eds) *Annotated catalogue of the Hymenoptera of Russia. Volume II. Apocrita: Parasitica. Proceedings of the Zoological Institute Russian Academy of Sciences. Supplement 8*. St Petersburg, 28–29.
- Liang L-H (2011) *Biodiversity in China's Yunnan province*. United Nations University. <https://unu.edu/publications/articles/biodiversity-in-chinas-yunnan-province.html> [Retrieved 25 October 2020]
- Liu Z, Yang SJ, Wang YY, Peng YQ, Chen HY, Luo SX (2021) Tackling the taxonomic challenges in the family Scoliidae (Insecta, Hymenoptera) using an integrative approach: A case study from southern China. *Insects* 12: e892. <https://doi.org/10.3390/insects12100892>

- Mo W-H, Chen H-Y, Pang H, Liu J-X (2021) DNA barcoding for molecular identification of the genus *Oxyscelio* (Hymenoptera, Scelionidae) from southern China, with descriptions of five new species. In: Lahey Z, Talamas E (Eds) Advances in the Systematics of Platygastroidea III. Journal of Hymenoptera Research 87: 613–633. <https://doi.org/10.3897/jhr.87.71912>
- Olmi M, Chen H-Y, Guglielmino A, Ødegaard F, Vollaro M, Capradossi L, Liu J-X (2022) DNA barcoding of *Aphelopus* Dalman (Hymenoptera, Dryinidae) from China, with descriptions of four new species. European Journal of Taxonomy 794: 40–71. <https://doi.org/10.5852/ejt.2022.794.1653>
- Peters RS, Krogmann L, Mayer C, Donath A, Gunkel S, Meusemann K, Kozlov A, Podsiadlowski L, Petersen M, Lanfear R, Diez PA, Heraty J, Kjer KM, Klopstein S, Mejer R, Polidori C, Schmitt T, Liu SL, Zhou X, Wappler T, Rust J, Misof B, Niehuis O (2017) Evolutionary history of the Hymenoptera. Current Biology 27(7): 1013–1018. <https://doi.org/10.1016/j.cub.2017.01.027>
- Puillandre N, Lambert A, Brouillet S, Achaz G (2012) ABGD, automatic barcode gap discovery for primary species delimitation. Molecular Ecology 21: 1864–1877. <https://doi.org/10.1111/j.1365-294X.2011.05239.x>
- Raff JW (1934) Observations on sawflies of the genus *Perga*, with notes on some reared primary parasites of the families Trigonalidae, Ichneumonidae, and Tachinidae. Proceedings of the Royal Society of Victoria 47: 54–77.
- Santos BF, Aguiar AP, Tedesco AM (2012) Trigonalidae (Hymenoptera) from cacao agroforestry systems in northeastern Brazil, with two new species of *Trigonalys* Westwood. Journal of Hymenoptera Research 25: 19–34. <https://doi.org/10.3897/jhr.25.1810>
- Smith DR, Janzen DH, Hallwachs W, Smith AM (2012) Hyperparasitoid wasps (Hymenoptera, Trigonalidae) reared from dry forest and rain forest caterpillars of Area de Conservación Guanacaste, Costa Rica. Journal of Hymenoptera Research 29(2012): 119–144. <https://doi.org/10.3897/jhr.29.3233>
- Smith DR, Stocks IC (2005) A new trigonalid wasp (Hymenoptera: Trigonalidae) from eastern North America. Proceedings of the Entomological Society of Washington 107: 530–535.
- Smith DR, Tripotin P (2012) Trigonalidae (Hymenoptera) of Madagascar. Journal of Hymenoptera Research 24: 1–25. <https://doi.org/10.3897/jhr.24.1811>
- Smith DR, Tripotin P (2015) Trigonalidae (Hymenoptera) of Thailand, other southeastern Asian records, and a new *Trigonalys* from India. Journal of Hymenoptera Research 44: 1–18. <https://doi.org/10.3897/jhr.44.4495>
- Talamas EJ, Bon M-C, Hoelmer KA, Buffington ML (2019) Molecular phylogeny of *Trissolcus* wasps (Hymenoptera, Scelionidae) associated with *Halyomorpha halys* (Hemiptera, Pentatomidae). In: Talamas E (Ed.) Advances in the Systematics of Platygastroidea II. Journal of Hymenoptera Research 73: 201–217. <https://doi.org/10.3897/jhr.73.39563>
- Tan J-L, van Achterberg C, Tan Q-Q, Zhao L-P (2017) New species of Trigonalidae (Hymenoptera) from NW China. ZooKeys 698: 17–58. <https://doi.org/10.3897/zookeys.698.13366>
- Weinstein P, Austin AD (1991) The host relationships of trigonalid wasps (Hymenoptera: Trigonalidae), with a review of their biology and catalogue to world species. Journal of Natural History 25(2): 399–433. <https://doi.org/10.1080/00222939100770281>

- Weinstein P, Austin AD (1995) Primary parasitism, development and adult biology in the wasp *Taeniogonalos venatoria* Riek (Hymenoptera: Trigonalidae). Australian Journal of Zoology 43: 541–555. <https://doi.org/10.1071/ZO9950541>
- Yamane S (2014) New taxa of the genus *Bareogonalos* from Asia with further information on the tribe Nomadinini (Hymenoptera, Trigonalidae). Halteres 5: 17–31. <https://doi.org/10.1016/j.aspen.2013.09.004>
- Yamane S, Terayama M (1983) Description of a new subspecies of *Bakeronymus typicus* Rohwer parasitic on the social wasp *Parapolybia varia* Fabricius in Taiwan (Hymenoptera: Trigonalidae). Memoirs of the Kagoshima University Research Center for the South Pacific 3: 169–173.
- Zhang J, Kapli P, Pavlidis P, Stamatakis A (2013) A general species delimitation method with applications to phylogenetic placements. Bioinformatics 29: 2869–2876. <https://doi.org/10.1093/bioinformatics/btt499>

Supplementary material 1

Table S1

Authors: Bing-Lan Zhang, Cheng-Jin Yan, Cornelis van Achterberg, Yan-Qiong Peng, Hua-Yan Chen

Data type: Specimen collecting information.

Explanation note: Details of sequenced specimens.

Copyright notice: This dataset is made available under the Open Database License (<http://opendatacommons.org/licenses/odbl/1.0/>). The Open Database License (ODbL) is a license agreement intended to allow users to freely share, modify, and use this Dataset while maintaining this same freedom for others, provided that the original source and author(s) are credited.

Link: <https://doi.org/10.3897/jhr.90.80150.suppl1>

Supplementary material 2

Table S2

Authors: Bing-Lan Zhang, Cheng-Jin Yan, Cornelis van Achterberg, Yan-Qiong Peng, Hua-Yan Chen

Data type: Genetic distances.

Explanation note: Genetic distance of COI within species under K2P model.

Copyright notice: This dataset is made available under the Open Database License (<http://opendatacommons.org/licenses/odbl/1.0/>). The Open Database License (ODbL) is a license agreement intended to allow users to freely share, modify, and use this Dataset while maintaining this same freedom for others, provided that the original source and author(s) are credited.

Link: <https://doi.org/10.3897/jhr.90.80150.suppl2>

Supplementary material 3

Table S3

Authors: Bing-Lan Zhang, Cheng-Jin Yan, Cornelis van Achterberg, Yan-Qiong Peng, Hua-Yan Chen

Data type: Interspecific pairwise distance.

Explanation note: Interspecific pairwise distance of Trygonalyidae based on COI sequences (%).

Copyright notice: This dataset is made available under the Open Database License (<http://opendatacommons.org/licenses/odbl/1.0/>). The Open Database License (ODbL) is a license agreement intended to allow users to freely share, modify, and use this Dataset while maintaining this same freedom for others, provided that the original source and author(s) are credited.

Link: <https://doi.org/10.3897/jhr.90.80150.suppl3>

Supplementary material 4

Figures

Authors: Bing-Lan Zhang, Cheng-Jin Yan, Cornelis van Achterberg, Yan-Qiong Peng, Hua-Yan Chen

Data type: Images.

Explanation note: Supplement figures of known Trygonalyidae species.

Copyright notice: This dataset is made available under the Open Database License (<http://opendatacommons.org/licenses/odbl/1.0/>). The Open Database License (ODbL) is a license agreement intended to allow users to freely share, modify, and use this Dataset while maintaining this same freedom for others, provided that the original source and author(s) are credited.

Link: <https://doi.org/10.3897/jhr.90.80150.suppl4>